Supporting Information

Naphthalene Diimide-based Random Terpolymers with Axisymmetric and Asymmetric Electron Acceptors for Controllable Morphology and Enhanced Fill Factors in All-Polymer Solar Cells

Geunhyung Park,[a, †] Yongjoon Cho,[a, e, †] Seunglok Lee,[a] Seungju Kim[d], Kyu Cheol Lee,[c, d,*] Changduk Yang[a, b, *]

Experimental Section

Materials and Measurements: All starting materials were purchased from Sigma-Aldrich, or TCI and used without further purification. All solvents are ACS and anhydrous grade unless otherwise noted. All dibrominated accepting monomers consisting a family of NDI-based copolymers, namely 4,9-Dibromo-2,7-bis(2-octyldodecyl)benzo[*lmn*][3,8]phenanthroline-1,3,6,8(2*H*,7*H*)-tetrone (NDI-Br_2), 1,3-dibromo-5,7-bis(2-ethylhexyl)-4H,8H-benzo[1,2-*c*:4,5-*c*']dithiophene-4,8-dione (BDD- Br_2), 1,3-dibromo-5-(2-hexyldecyl)-4*H*-thieno[3,4-*c*]pyrrole-4,6(5*H*)-dione (TPD- Br_2), 2-ethylhexyl 4,6-dibromo-3-fluorothieno[3,4-*b*]thiophene-2-carboxylate (TT- Br_2), and 5,8-dibromo-6,7-difluoro-2-((2-hexyldecyl)oxy)quinoxaline (FTQ- Br_2) and their counter monomer, namely 5,5'-bis(trimethylstannyl)-2,2'-bithiophene (BT-Sn_2) were prepared according to the previously established synthetic procedures. [ref1-6] ^{1}H NMR spectra were recorded on a VNMRS 600 (Agilent, USA) spectrophotometer using 1,1,2,2-tetrachloroethane-d_2 as the solvent and tetramethylsilane as the internal standard (**Figures S**5-9). The number-average (M_n) and weight-average (M_w) molecular S-2weights, and the polydispersity indices (PDIs) of the polymer products were determined by high-temperature gel-permeation chromatography (HT-GPC) with Agilent 1200 HPLC and mini DAWN TREOS using polystyrene as the standard in 1,2,4-trichlorobenzene at 100 °C (HPLC grade). UV-Vis-NIR spectra were recorded on a UV-1800 (SHIMADZU) spectrophotometer. Cyclic voltammetry (CV) measurements were performed on a Solartron electrochemical station (METEK, Versa STAT3) with a three-electrode cell in a 0.1 M tetran-butylammonium hexafluorophosphate (*n*-Bu_4NPF_6) solution in acetonitrile at a scan rate of 100 mV s^{-1} at room temperature. An Ag/Ag^+ (0.01 M $AgNO_3$ in acetonitrile) electrode, a platinum wire, and a polymer-coated platinum electrode were used as the reference electrode, the counter electrode, and the working electrode, respectively. The Ag/Ag^+ reference electrode was calibrated using a ferrocene/ferrocenium redox couple as an internal standard, whose oxidation potential is set at − 4.8 eV with respect to the zero vacuum

level. The LUMO levels of the polymers were obtained from the equation ($E_{LUMO} = -(E_{red}^{onset} - E_{(ferrocene)}^{onset} + 4.8)$ (eV)). The HOMO energy levels were obtained from the equation ($E_{HOMO} = E_{LUMO} - E_g^{opt}$ (eV)). DFT calculations were performed using the Gaussian 09 package with the nonlocal hybrid Becke three-parameter Lee–Yang–Parr (B3LYP) function and the 6-31G* basis set to elucidate the dipole moment and energy levels after optimizing the geometries using the same method. Electron affinity (EA) is calculated with EA = E(M) – E(M^-), where E(M) and E(M^-) are the neutral, and anionic energies, respectively. E(M^-) is the energies of the optimized anionic structures, respectively.

General Procedure for PNDI-based Polymers Using Stille Couling: In a Schlenk flask, NDI-Br2 (a mol), monomers (b mols), and BT-Sn_2 (a + b mol, 1 eq) were dissolved in anhydrous toluene (10 mL) under Ar atmosphere. Then, Pd_2(dba)3 (0.03 eq) and P(*o*-tolyl)$_3$ (0.12 eq) were added and purged again with Ar gas for 10 min. After that, the reaction was stirred at 100 ℃ for 48 h, followed by the addition of small amounts of 2bromothiophene and 2-(trimethylstannyl)thiophene as the end-capping agent, respectively. The reaction mixture was cooled down to room temperature and precipitated to methanol. The precipitated crude solids were filtered and purified via Soxhlet extraction with methanol, acetone, hexane, and chloroform. The solute in chloroform solution was concentrated and precipitated to methanol again. The extracted copolymers were collected by filtration and dried in vacuum oven.

N2200: On basis of the general procedure described above, NDI-Br_2 (200 mg, 0.20 mmol) and BT-Sn_2 (98 mg, 0.20 mmol) were used for polymerization. Yield = 93 %. M_n = 51.5 kDa, PDI = 2.5. ^{1}H NMR (600 MHz, 80 ℃, 1,1,2,2-tetrachloroethane-d_2), δ (ppm): 8.92 – 8.86 (br), 7.46 – 7.38 (br), 4.29 – 4.09 (br), 2.13 – 2.04 (br), 1.55 – 1.20 (br), 0.97 – 0.85 (br). Elemental analysis: anal. calcd, C, 75.24; H, 8.98; N, 2.83; S, 6.48. Found: C, 75.17; H, 9.07; N, 2.55; S, 6.50.

P(NDI-BDD10): On basis of the general procedure described above, NDI-Br_2 (180 mg, 0.18 mmol), BDD-Br_2 (11 mg, 0.02 mmol), and BT-Sn_2 (98 mg, 0.20 mmol) were used for polymerization. Yield = 90 %. M_n = 72.4 kDa, PDI = 1.80. ^{1}H NMR (600 MHz, 80 ℃, 1,1,2,2-tetrachloroethane-d_2), δ (ppm): 8.92 – 8.86 (br), 7.88 – 7.84 (br), 7.46 – 7.38 (br), 7.38 – 7.34 (br) 4.29 – 4.09 (br), 3.48 – 3.38 (br), 2.17 – 2.01 (br), 1.92 – 1.82 (br), 1.66 – 1.11 (br), 1.07 – 1.02 (br), 0.99 – 0.95 (br), 0.95 – 0.85 (br). Elemental analysis: anal. calcd, C, 74.45; H, 8.71; N, 2.55; S, 7.94. Found: C, 74.73; H, 8.91; N, 2.51; S, 8.01.

P(NDI-TPD10): On basis of the general procedure described above, NDI-Br_2 (180 mg, 0.18 mmol), TPD-Br_2 (10 mg, 0.02 mmol), and BT-Sn_2 (98 mg, 0.20 mmol) were used for polymerization. Yield = 95 %. M_n = 69.7 kDa, PDI = 1.80. ^{1}H NMR (600 MHz, 80 ℃, 1,1,2,2-tetrachloroethane-d_2), δ (ppm): 8.94 – 8.81 (br), 8.13 – 8.06 (br), 7.85 – 7.81 (br), 7.67 – 7.63 (br), 7.55 – 7.38 (br), 7.38 – 7.31 (br), 4.33 – 4.03 (br), 2.97 – 2.90 (br), 2.19 – 2.01 (br), 1.73 – 1.11 (br), 1.05 – 0.78 (br). Elemental analysis: anal. calcd, C, 74.39; H, 8.77; N, 2.81; S, 7.61. Found: C, 74.84; H, 8.84; N, 2.80; S, 7.67.

P(NDI-TT10): On basis of the general procedure described above, NDI-Br_2 (180 mg, 0.18 mmol), TT-Br_2 (9 mg, 0.02 mmol), and BT-Sn_2 (98 mg, 0.20 mmol) were used for polymerization. Yield = 91 %. M_n = 68.9 kDa, PDI = 1.69. ^{1}H NMR (600 MHz, 80 ℃, 1,1,2,2-tetrachloroethane-d_2), δ (ppm): 8.92 – 8.86 (br), 7.50 – 7.38 (br), 7.38 – 7.32 (br), 4.42 – 4.31 (br), 4.29 – 4.03 (br), 2.17 – 1.98 (br), 1.86 – 1.71 (br), 1.67 – 1.15 (br), 1.08 – 0.77 (br). Elemental analysis: anal. calcd, C, 73.51; H, 8.53; N, 2.55; S, 8.52. Found: C, 73.87; H, 8.60; N, 2.53; S, 8.57.

P(NDI-FTQ10): On basis of the general procedure described above, NDI-Br_2 (180 mg, 0.18 mmol), FTQ-Br_2 (10 mg, 0.02 mmol), and BT-Sn_2 (98 mg, 0.20 mmol) were used for polymerization. Yield = 90 %. M_n = 72.5 kDa, PDI = 1.71. ^{1}H NMR (600 MHz, 80 ℃, 1,1,2,2-tetrachloroethane-d_2), δ (ppm): 8.92 – 8.86 (br), 8.76 – 8.66 (br), 8.07 – 8.02 (br), 7.52 – 7.33 (br), 4.77 – 4.67 (br), 4.29 – 4.09 (br), 2.17 – 2.01 (br), 1.68 – 1.12 (br), 1.05 – 0.77 (br). Elemental analysis: anal. calcd, C, 74.47; H, 8.76; N, 3.04; S, 6.96. Found: C, 74.55; H, 8.85; N, 3.01; S, 6.98.

Morphology Characterization: The investigation of thin-film morphology was performed using AFM, TEM, contact angles, and GIWAXS measurements. The samples were prepared by spin-coating on the glass substrate (for AFM and TEM) or silicon substrate (for GIWAXS) using the solution of NFAs (2 mg mL^{-1} in CF) for the neat film and the optimized device fabrication condition for the blend films. AFM and TEM were measured via a Hitachi AFM5100N in the tapping mode and Tecnai G2 F20 X-Twin transmission electron microscope equipped with an energy-dispersive X-ray analysis at an acceleration voltage of 200 kV, respectively. The contact angle test was performed on a Phoenix 300 (SEO), and the surface energy of the acceptors and PM6 was evaluated by measuring the contact angles using two different solvents: DI water and ethylene glycol (EG) on each neat film and calculated via the Owens−Wendt model. The corresponding blend miscibility between the donor and acceptor was estimated by the Flory−Huggins interaction parameter (χ) calculated by the following equation. GIWAXS analysis was conducted using a PLS-II 6D and 9A U-SAXS beamline in Pohang Accelerator Laboratory (South Korea). The X-rays coming from the in-vacuum undulator (IVU) were monochromated at 11.05 keV (wavelength of 1.12199 Å). The X-ray beam was irradiated with an incidence angle of <0.14° and for 1−30 s. GIXD patterns were recorded by a 2D CCD detector with a sample-to-detector distance (SDD) of 222.0 mm. The approximate crystalline coherence length (CCL) was extracted using the Scherrer equation

The GIWAXS measurement was carried out at the PLS-II 6D U-SAXS beamline of the Pohang Accelerator Laboratory in Korea. The X-rays coming from the in-vacuum undulator (IVU)

were monochromated (wavelength λ = 1.07212 A) using a double crystal monochromator and focused both horizontally and vertically (450 (H) × 60 (V) μm2 in FWHM @ the sample position) using K-B type mirrors. The grazing incidence wide-angle X-ray scattering (GIWAXS) sample stage was equipped with a 7-axis motorized stage for the fine alignment of the sample, and the incidence angles of the X-ray beam were set to be 0.13° for the blend films. The GIWAXS patterns were recorded with a 2D CCD detector (Rayonix SX165) and an X-ray irradiation time within 100 s, dependent on the saturation level of the detector. Diffraction angles were calibrated using a sucrose standard (monoclinic, P21, a = 10.8631 A, b = 8.7044 A, c = 7.7624 A, and β = 102.938°) and the sample-to-detector distance was ≈227 mm. The thickness of the films was measured using a stylus profilometer (P6, KLA Tencor). The approximate crystalline coherence length (CCL) was extracted using the Scherrer equation.

$$CCL = \frac{K\lambda}{\beta \cdot cos\,\theta} \tag{1}$$

where K is the Scherrer constant, λ is the wavelength (nm) if the X-ray beam used, β is the fill width at half-maximum, and θ is the Bragg angle.

Device Fabrication and Measurement: The OSC devices were fabricated with the conventional configuration of glass/ITO/PEDOT:PSS/active layer/PDINO/Al. The patterned ITO–coated glass substrate was cleaned using detergent, DI water, acetone, and isopropanol for 15 min for each step, subsequently. After the ITO glass substrates were treated with UV−ozone for 15 min, PEDOT:PSS (Bayer Baytron 4083) was spin-coated at 4000 rpm onto the ITO substrate, followed by annealing at 150 °C for 20 min in air. The PBDB-T:polymer acceptor (1:1 weight ratio) were dissolved in chlorobenzene at a concentration of 20 mg mL^{-1} with 0.5vol % of 1,8–diiodooctane as an additive and stirred on a hotplate heated at 50 ℃ for 3 h. The blend solution was spin-coated onto the PEDOT:PSS. Then, a methanol solution of PDINO (1.0 mg mL^{-1}) was deposited onto the active layer via spin–coating at 3000 rpm for 30 s. Finally, 100 nm Al was thermally evaporated under vacuum (<3.0 × 10^{-6} Pa). The *J–V* characteristics were measured on a Keysight B2900 sourcemeter under the illumination of an AM 1.5G solar simulator with an intensity of 100 mW cm−2. The EQE measurements were conducted using a Model QE-R3011 (Enli Technology) in ambient air. The hole and electron mobilities were measured using the SCLC method. Device structures are ITO/PEDOT:PSS/photoactive layer/Au for hole-only devices and ITO/ZnO/photoactive layer/PDINO/Al for electron-only devices. The SCLC mobilities were calculated using the Mott−Gurney equation

$$j = \frac{9}{8}\varepsilon_0\varepsilon_r\mu\left(\frac{V^2}{L^3}\right) \tag{2}$$

where ε_0 is the permittivity of empty space, ε_r is the relative dielectric constant of the organic semiconductor, μ is the mobility of zero-field, V is the applied voltage across the device, and L is the thickness of the active layer.

Table S1. Dipole moment, LUMO level and adiabatic EA for accepting units

	Vector			Dipole Moment (D)	E_{LUMO}^{DFT} (eV)	$EA_{adiabatic}$ (eV)
	x	y	z			
NDI	0.00	0.00	0.00	0.00	-3.78	2.70
BDD	0.00	-0.83	0.00	0.83	-2.48	1.30
TPD	0.00	-2.09	0.00	2.09	-2.20	0.85
TT	-1.56	-1.48	0.00	2.15	-2.23	1.18
2FQ	-1.36	4.01	0.00	4.23	-2.46	1.22

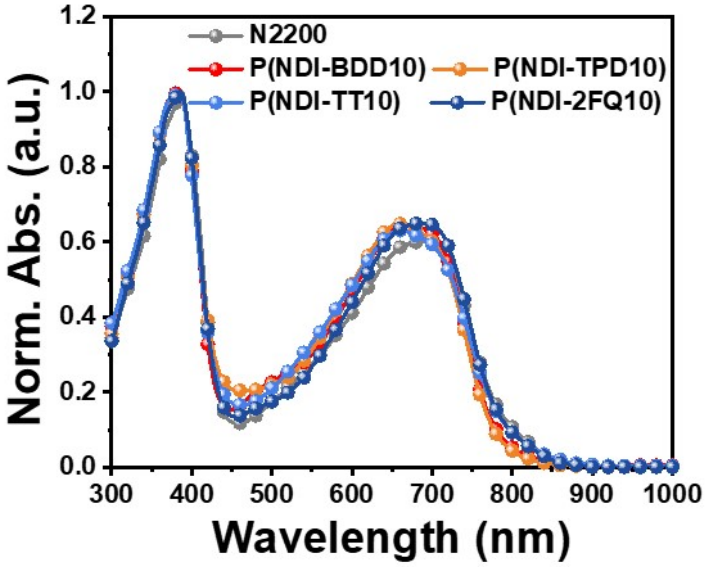

Figure S1. Normalized UV-Vis absorption spectra in chloroform.

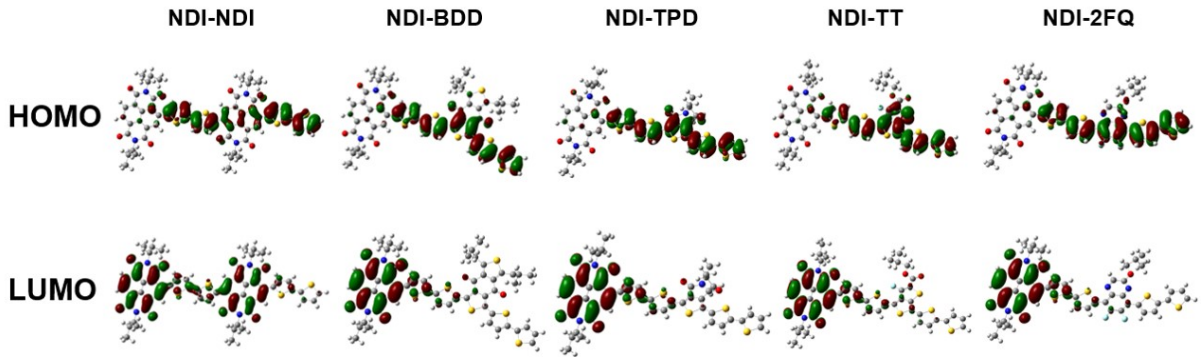

c

Figure S2. Simulated HOMO and LUMO distributions by DFT calculation.

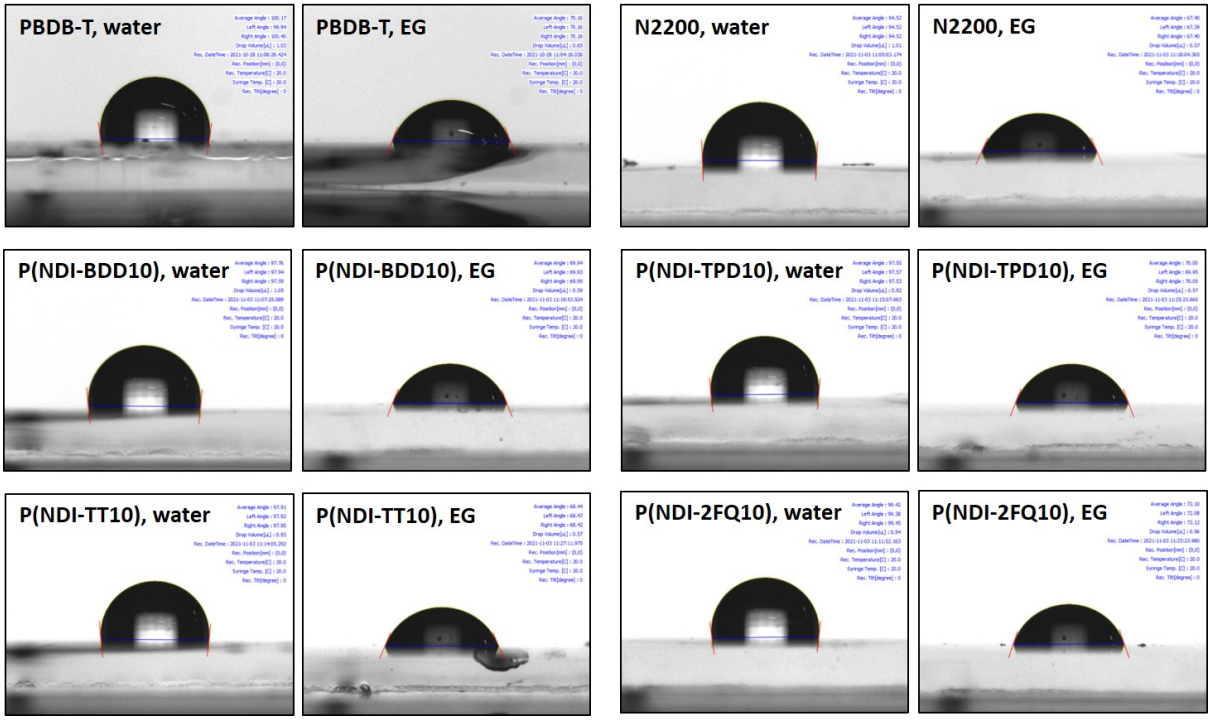

Figure S3. Contact angle images.

Table S2. Contact angles, calculated surface energies, and Flory-Huggins interaction parameter

	Contact angle [°]		Surface energy [mJm^{-2}]			
	Water	Ethylene glycol	γ^d	γ^p	γ^{total}	χ
PBDB-T	100.17	70.16	22.00	4.38	26.38	-
N2200	94.52	67.4	17.36	8.25	25.61	0.0057
P(NDI-BDD10)	97.76	69.94	18.50	6.46	24.96	0.0196
P(NDI-TPD10)	97.55	70.0	18.15	6.68	24.83	0.0235
P(NDI-TT10)	97.91	68.44	20.58	5.68	26.26	0.0001
P(NDI-2FQ10)	99.42	72.1	18.16	5.93	24.09	0.0520

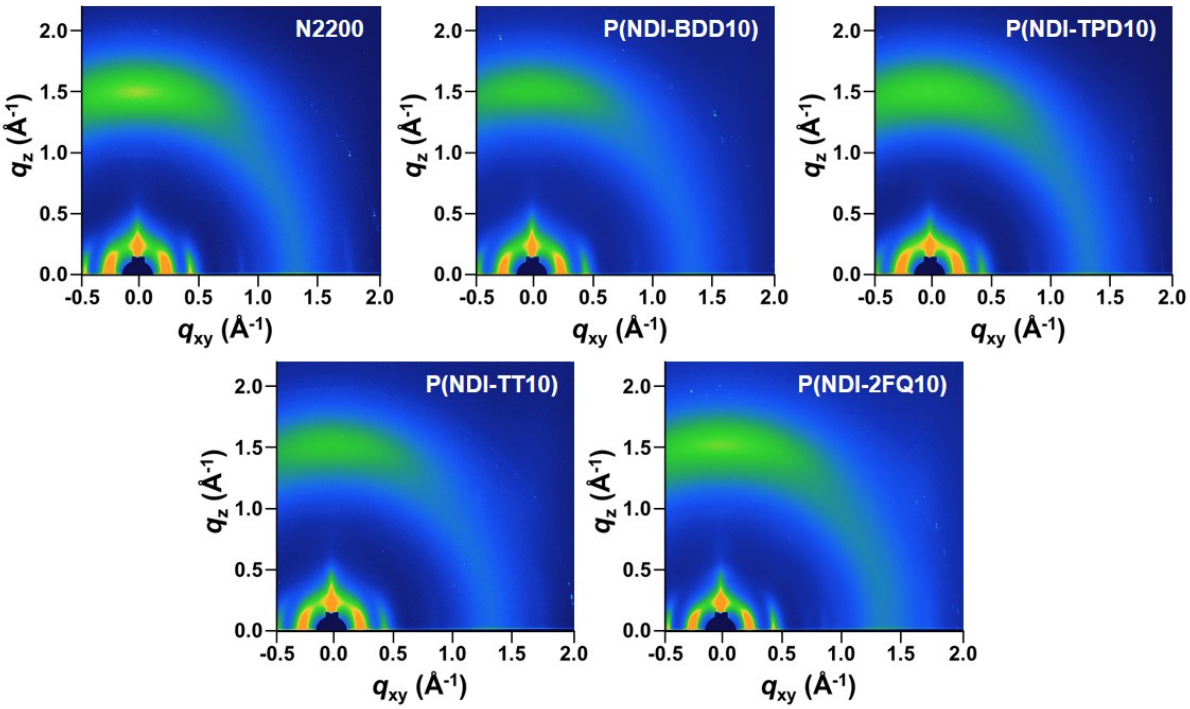

Figure S4. 2D-GIWAXS images of the neat films.

Table S3. GIWAXS parameters of the blend films

Crystallographic parameters		In-plane (100)	In-plane (200)	OOP (100)	OOP (010)
PBDB-T:N2200	q (Å^{-1})	0.289	0.470	0.299	1.656
	d-spacing (Å)	21.7	13.4	21.0	3.8
	FWHM (Å^{-1})	0.058	0.043	0.089	0.305
	Coherence length (Å)	97.8	131.6	63.3	18.7
PBDB-T: P(NDI-BDD10)	q (Å^{-1})	0.287	0.471	0.308	1.638
	d-spacing (Å)	21.9	13.4	20.4	3.8
	FWHM (Å^{-1})	0.055	0.035	0.065	0.283
	Coherence length (Å)	103.2	162.7	86.9	20.2
PBDB-T: P(NDI-TPD10)	q (Å^{-1})	0.285	0.467	0.311	1.653
	d-spacing (Å)	22.0	13.4	20.2	3.8
	FWHM (Å^{-1})	0.061	0.042	0.065	0.288
	Coherence length (Å)	93.2	134.4	86.7	19.9
PBDB-T: P(NDI-TT10)	q (Å^{-1})	0.285	0.467	0.297	1.653
	d-spacing (Å)	22.1	13.5	21.2	3.8
	FWHM (Å^{-1})	0.062	0.041	0.081	0.303
	Coherence length (Å)	91.7	136.6	69.8	18.9
PBDB-T: P(NDI-2FQ10)	q (Å^{-1})	0.282	0.469	0.292	1.649
	d-spacing (Å)	22.3	13.4	21.5	3.8
	FWHM (Å^{-1})	0.062	0.041	0.076	0.296
	Coherence length (Å)	91.6	138.9	74.7	19.3

Table S4. Hole and electron mobility of the OSC devices.

	μ_h (cm^2 V^{-1} S^{-1})	μ_e (cm^2 V^{-1} S^{-1})	μ_e / μ_h
PBDB-T:N2200	2.00×10^{-4}	1.77×10^{-4}	0.884
PBDB-T:P(NDI-BDD10)	2.43×10^{-4}	2.41×10^{-4}	0.991
PBDB-T:P(NDI-TPD10)	2.34×10^{-4}	2.11×10^{-4}	0.899
PBDB-T:P(NDI-TT10)	1.50×10^{-4}	7.35×10^{-5}	0.491
PBDB-T:P(NDI-2FQ10)	2.16×10^{-4}	1.98×10^{-4}	0.918

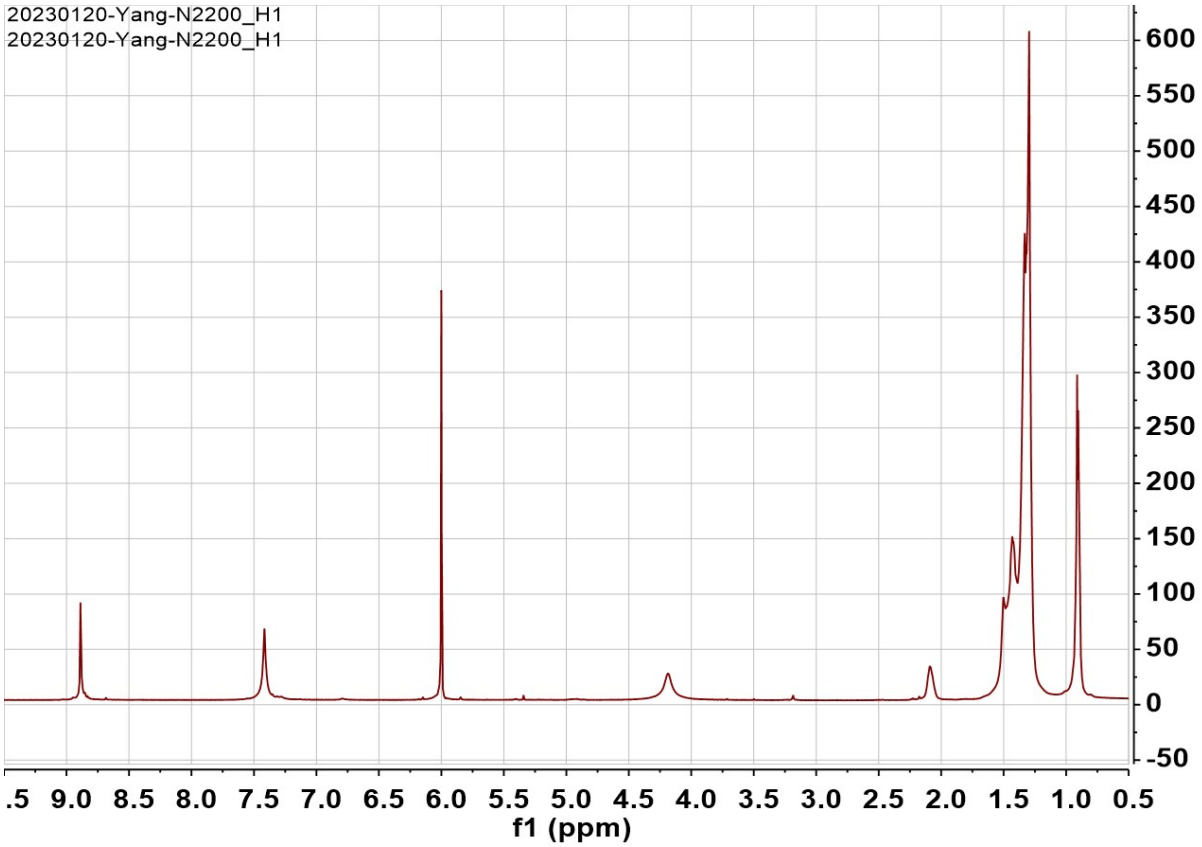

Figure S5. ^{1}H NMR spectrum of N2200.

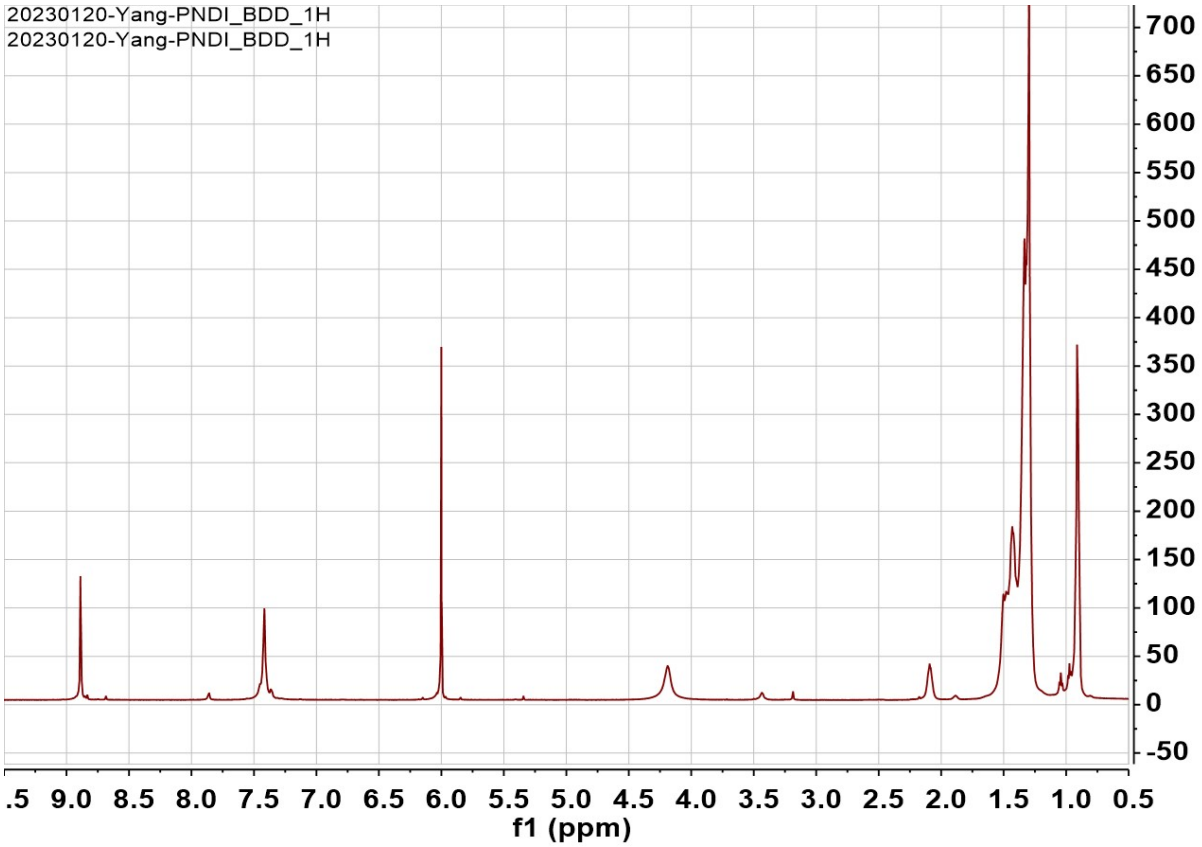

Figure S6. ^{1}H NMR spectrum of P(NDI-BDD10).

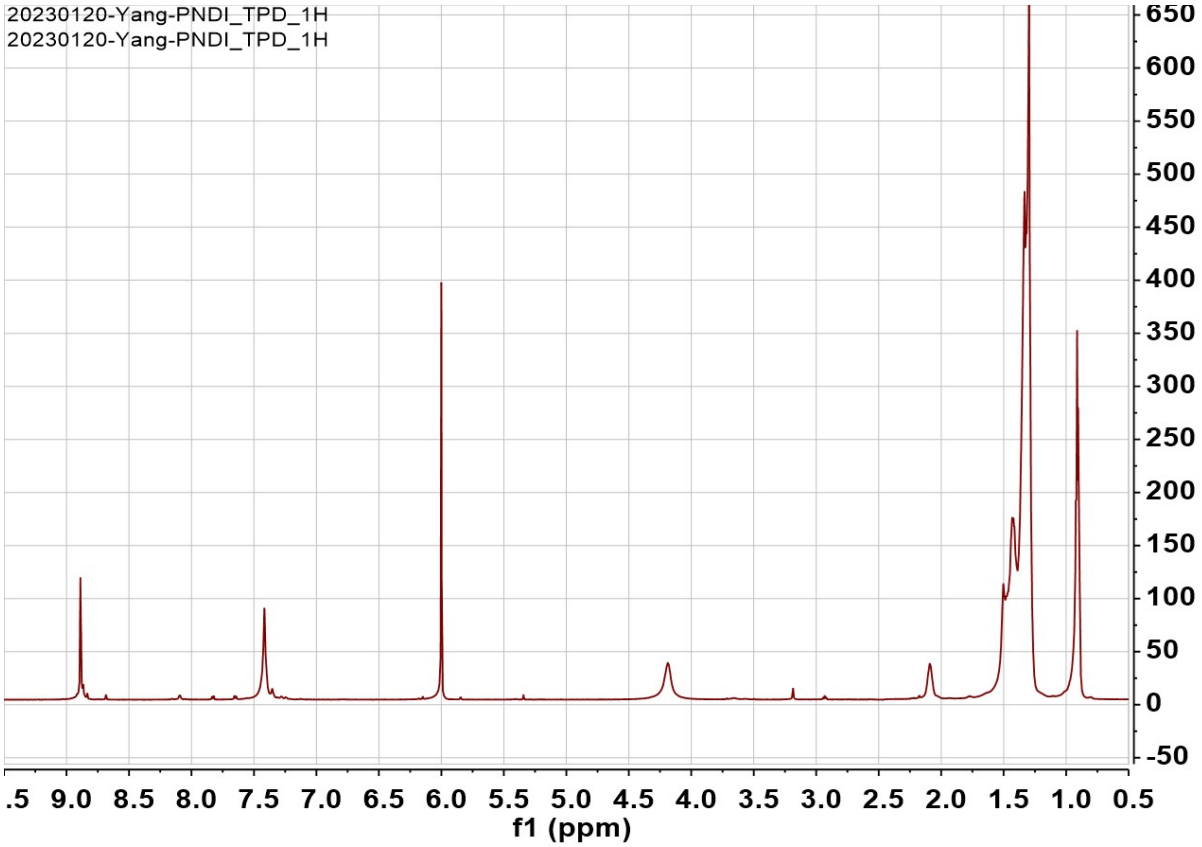

Figure S7. ^{1}H NMR spectrum of P(NDI-TPD10).

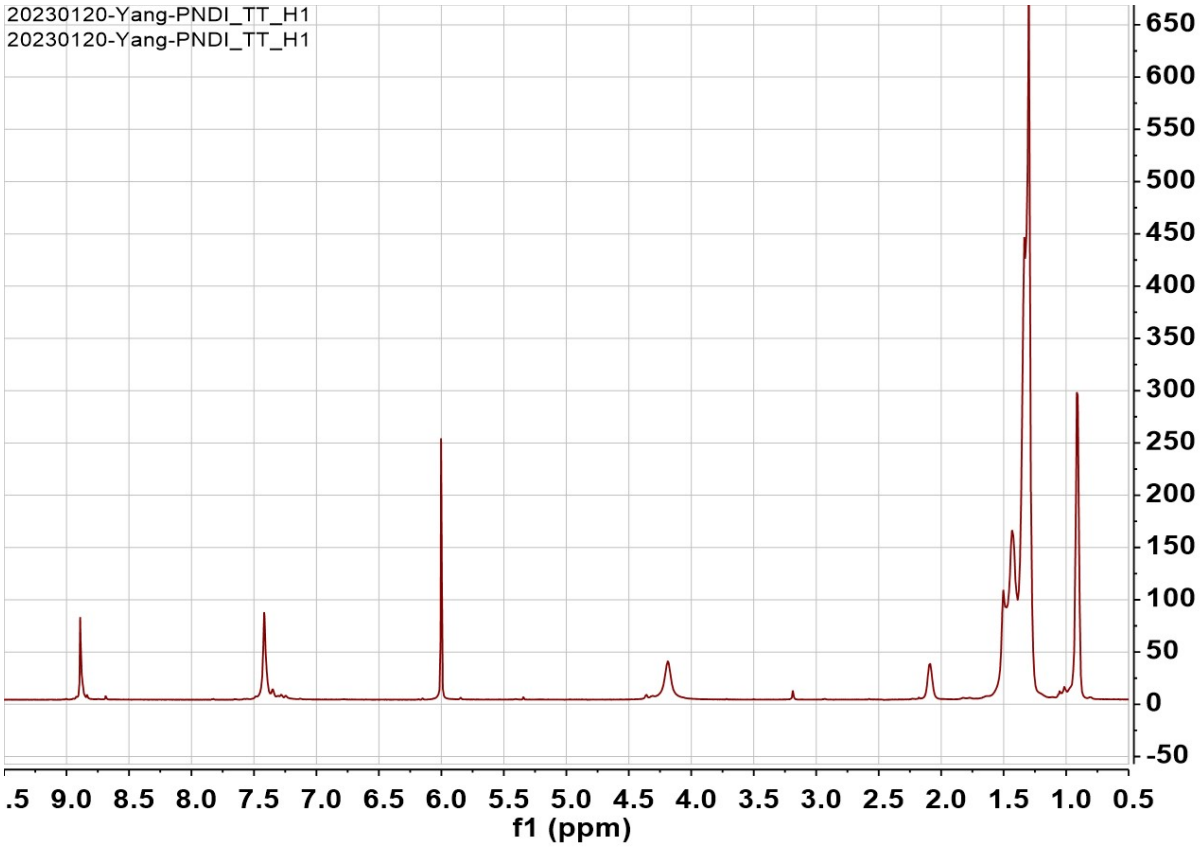

Figure S8. ^{1}H NMR spectrum of P(NDI-TT10).

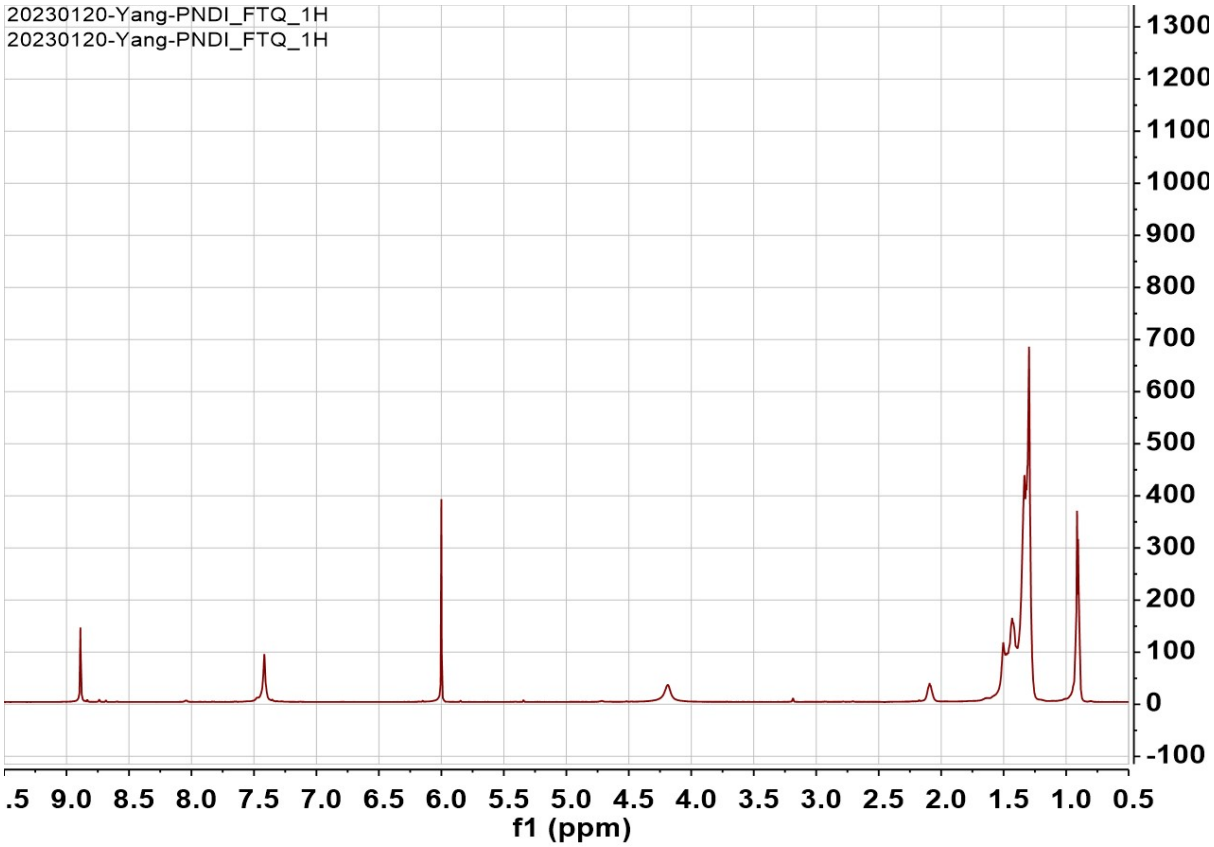

Figure S9. ^{1}H NMR spectrum of P(NDI-FTQ10).

Reference

1. X. Guo, F. S. Kim, M. J. Seger, S. A. Jenekhe and M. D. Watson, *Chem. Mat.*, 2012, **24**, 1434-1442.
2. J. W. Jo, J. W. Jung, H.-W. Wang, P. Kim, T. P. Russell and W. H. Jo, *Chem. Mat.*, 2014, **26**, 4214-4220.
3. Y. Liang, D. Feng, Y. Wu, S.-T. Tsai, G. Li, C. Ray and L. Yu, *J. Am. Chem. Soc.*, 2009, **131**, 7792-7799.
4. A. Najari, S. Beaupré, P. Berrouard, Y. Zou, J.-R. Pouliot, C. Lepage-Pérusse and M. Leclerc, *Adv. Funct. Mater.*, 2011, **21**, 718-728.
5. D. Qian, L. Ye, M. Zhang, Y. Liang, L. Li, Y. Huang, X. Guo, S. Zhang, Z. a. Tan and J. Hou, *Macromolecules*, 2012, **45**, 9611-9617.
6. C. Sun, F. Pan, H. Bin, J. Zhang, L. Xue, B. Qiu, Z. Wei, Z.-G. Zhang and Y. Li, *Nat. Commun.*, 2018, **9**, 743.